

## INFLUENCE OF THE INLET CONDITIONS ON THE DEGREE OF MIXING OF A T-SHAPED MICRO-MIXER

Galletti C.\* Brunazzi E. and Mauri R.

\*Author for correspondence

Department of Chemical Engineering, Industrial Chemistry and Materials Science

University of Pisa,

Pisa, I-56126,

Italy

E-mail: chiara.galletti@diccism.unipi.it

### ABSTRACT

The degree of mixing of a T-shaped micro-mixer depends strongly on the inlet flow conditions. Specifically, through a series of numerical simulations, we compared the case where the flow at the micro-mixer confluence is fully developed with that when it is not, and found that in the former case engulfment occurs at smaller Reynolds number, with a different flow pattern and with much larger mixing efficiencies than in the latter case. In particular for fully developed flow conditions the engulfment shows S-shaped morphology, whereas for non-fully developed inlets a symmetry breaking occurs, leading to a C-shaped engulfment pattern. This is characterized by much lower mixing efficiencies.

### INTRODUCTION

Recently, great attention has been devoted to understanding the governing mechanisms and optimising the performance of micro-mixers. Among them, passive micro-mixers are especially interesting as they promote mixing without the help of any external power, through stretching and recombining of the flow fields [1].

T or Y shapes, in which the inlets join the main channel with T- or Y-shaped branches, are the simplest micro-mixer geometries. These are also suitable to shed light into fundamental aspects; moreover the T-shaped micro-mixer is a junction element often involved in more complex micro-systems [2].

The efficiency of T-shaped micro-mixers for liquid mixing has been proved by [3] who used such devices to quench down a chemical reaction in a very short time. Lately, [4] [5] and [6] showed that three different flow regimes occur in the micro-mixer, depending on the Reynolds number,  $Re$ , namely: the laminar, vortex and engulfment flow regimes.

### NOMENCLATURE

A	[m <sup>2</sup> ]	area
c	[-]	normalised concentration
$\bar{c}$	[-]	mean concentration
$D_{h,in}$	[m]	hydraulic diameter of the inlet channels
G	[Pa/m]	pressure gradient
H	[m]	depth of all the channels
k	[-]	index
L	[m]	mixing channel length
L'	[m]	inlet channel length
Le	[m]	length to reach fully developed conditions
Pe	[-]	Peclet number
Re	[-]	Reynolds number in the mixing channel
$Re_{in}$	[-]	Reynolds number in the inlet channel
Sc	[-]	Schmidt number
v	[m/s]	velocity
$\bar{v}$	[m/s]	mean velocity
W	[m]	width of the mixing channel
W'	[m]	width of the inlet channels
x, y, z	[m]	spatial coordinates
Y	[m]	conduit width
Z	[m]	conduit height

#### Greek symbols

$\delta_m$	[-]	degree of mixing
$\overline{(\Delta c)^2}$	[-]	mean square concentration difference,
$\eta$	[-]	conduit aspect ratio
$\mu$	[kg/(m s)]	dynamic viscosity
$\rho$	[kg/m <sup>3</sup> ]	density
$\sigma_{cm}^2$	[-]	cup mixing flow variance

#### Subscripts

i	indices
x,y,z	directions
max	maximum

#### Abbreviations

CFD	Computational Fluid Dynamics
FD	Fully Developed
O	order of

In the laminar flow regime the inlet streams come into contact with one another in the mixing zone and then flow side by side through the mixing channel, resulting in a completely segregated flow (stratified flow). In the vortex regime, above a critical  $Re$ , a secondary flow in the form of a double vortex pair occurs, due to the instabilities induced by the centrifugal forces at the confluence. In the engulfment regime occurring at higher  $Re$ , fluid elements reach the opposite side of the mixing channel, thus largely increasing the degree of mixing. For a micro-mixer having a mixing channel with  $W = 2 W'$  and  $W' = H = 100 \mu\text{m}$ , the engulfment occurred at  $Re = 146$  [4] [6]. Subsequently, in order to ensure fast and efficient liquid mixing it is clearly fundamental to work in the engulfment flow regime and thus at relatively high  $Re$ . This is why several investigations were aimed at assessing the effect of different geometric and operating parameters on the engulfment process [7] [8].

In recent research contributions, Computational Fluid Dynamics (CFD) was extensively used to evaluate mixing performance or propose design upgrading [6] [9] [10] [11]; in fact, CFD calculations have been found to give encouraging results when compared to experimental data, mainly because in laminar conditions and with small size devices no additional models have to be used and basically the CFD solver is employed as a Navier-Stokes equation integrator. However, a few researchers highlighted the importance of a careful choice of the discretization process to obtain reliable results and indicated the need of very fine (and thus CPU time costing) computational grids, even though lots of investigations were performed with coarser grids [12], thus yielding unrealistic predictions.

The present paper aims at analyzing the effect of the inlet flow conditions on the engulfment, as this has not been investigated in literature, yet. Our motivation stems from the fact that in the engulfment regime the inlet channels could not be sufficiently long to ensure that at the junction of the T-mixer the inlet flow is fully developed, as it is generally assumed to be. For example, in the case of micro-channel networks, of which T-shaped micro-mixers are the basic elements, there can be limitations on the inlet channel a length, preventing the inlet flows from being fully developed.

## TEST CASES

The T-shaped micro-mixer and the reference coordinate system are depicted in Figure 1. The micro-mixer has a mixing channel length  $L = 3000 \mu\text{m}$ , width  $W = 300 \mu\text{m}$  and depth  $H = 200 \mu\text{m}$ , while the inlet channels have a width  $W' = W/2 = 150 \mu\text{m}$  and a length  $L' = 1500 \mu\text{m}$ . The liquid is injected at the two inlets with the same flow rates. The inlet flow mean velocity was varied between 0.4 and 2.2 m/s, corresponding to mixing channel Reynolds number between 96 to 528.

Two hypotheses are made:

- the flow enters the inlets after a conduit that is long enough to reach fully developed (FD) flow conditions (FD case);
- the flow is injected at the inlets with an uniform velocity profile (non-FD case).

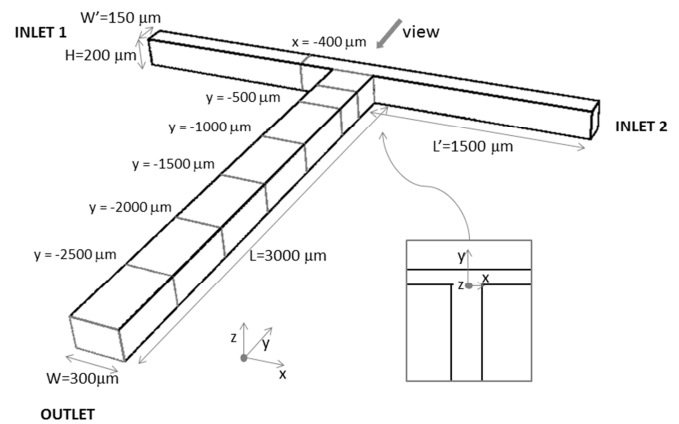


Figure 1 - Sketch of the T-shaped micro-mixer

## NUMERICAL METHOD

Simulations were performed with the commercial Ansys 13 code, using the FLUENT fluid dynamics package.

### Computational domain and grid

The grid was created with the software ICEM. A structured grid with regular cubical elements of  $4 \mu\text{m}$  edge (4.2 million elements) was chosen based on a grid independency study on the velocity field. Such a grid, although rather computationally expensive, was found to be necessary to capture the flow features. In a cross section of the mixing channel there are  $76 \times 50$  elements, thus in fully agreement with recommendations by [12].

### Physical model

The liquid is water at ambient conditions (density  $\rho = 998 \text{ kg/m}^3$ , viscosity  $\mu = 0.001 \text{ kg/m s}$ ). A tracer was injected from one inlet with a molecular diffusivity of  $3 \times 10^{-10} \text{ m}^2/\text{s}$ , corresponding to the value of the crystal violet dye. Since the Schmidt number  $Sc = O(10^4)$ , the Peclet number,  $Pe = Sc Re$  is of  $O(10^6)$ , indicating that mass transport is dominated by convection, so molecular diffusion can be neglected altogether and the solute can be considered as a passive tracer. For all practical purposes, the problem is equivalent to studying the mixing process of one water stream into with the other [13]. Therefore, in the following text  $c$  will denote either the normalized concentration (i.e. ranging from 0 to 1) of the solute or that of one of the two water streams. At the outlet of the mixing channel, the pressure was set equal to the ambient pressure, while no-slip boundary conditions were applied to the fixed walls. In addition, as mentioned above, velocity boundary conditions at both inlet sections, were:

- an uniform velocity profile (non-FD inlet case);
- a fully developed velocity profile in a rectangular conduit (FD inlet case).

The latter is found by solving the Navier-Stokes equations with no-slip boundary conditions at the walls in a rectangular conduit [14-15], obtaining:

$$v(y, z) = -\frac{G}{2\mu} y(Y - y) - \frac{4GY^2}{\mu\pi^3} \sum_{k \text{ odd}} \frac{1}{k^3} \sin\left(k\pi \frac{y}{Y}\right) \left[ \text{Cosh}\left(k\pi \frac{z}{Y}\right) - \text{Tanh}\left(\frac{k\pi}{2\eta}\right) \text{Sinh}\left(k\pi \frac{z}{Y}\right) \right] \quad (1)$$

where  $Y$  and  $Z$  are the sizes of the conduit (corresponding to  $W'$  and  $H$  in our case), while  $\eta$  is the conduit aspect ratio. The pressure gradient  $G$  can be derived as a function of the mean velocity  $\bar{v}$ , finding:

$$G = -\frac{12\mu\bar{v}}{Y^2} \left[ 1 - \frac{192}{\pi^5} \eta \sum_{k \text{ odd}} \frac{1}{k^5} \text{Tanh}\left(\frac{k\pi}{2\eta}\right) \right]^{-1} \quad (2)$$

The velocity profile of Eq. (1) was imposed at the inlet boundaries by defining an ad hoc C++ subroutine.

Figure 2 illustrates the impact of the two types of boundary conditions on the velocity profile at the entrance of the mixing zone ( $x = -400 \mu\text{m}$ ) for  $\text{Re} = 480$ . Such a region was evaluated from the analysis of the FD case as the region at which streamlines start to bend and deviate from the Poiseuille flow. It can be noticed that the non-FD case exhibits a flat region in the centre of the conduit, with a peak velocity which is about 15% lower than that for the FD case.

Such a difference is due to the fact that a  $1500 \mu\text{m}$  inlet channel is not long enough to ensure a fully developed flow for  $\text{Re} = 480$ . Indeed, the conduit length to hydraulic diameter ratio that is needed to reach fully developed conditions, for rectangular conduits can be evaluated as [16]:

$$\frac{L_e}{D_{h_{in}}} = 0.379 \exp(-0.148 \text{Re}_{in}) + 0.055 \text{Re}_{in} + 0.26 \quad (3)$$

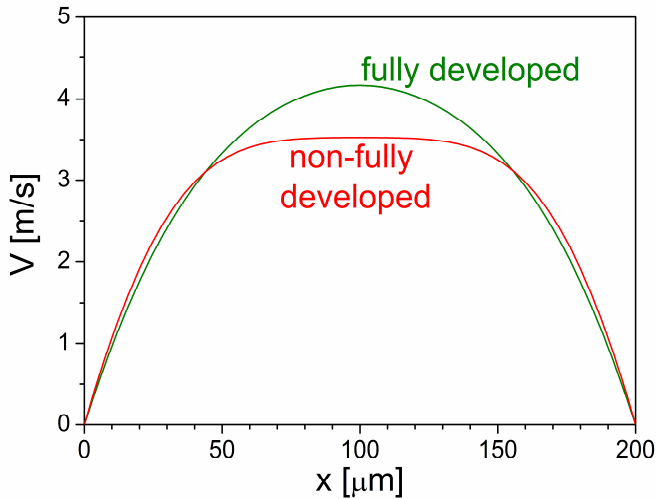


**Figure 2** - Longitudinal velocity ( $v_x$ ) profiles along the vertical centerline of the inlet channels at  $x = -400 \mu\text{m}$ .  $\text{Re} = 480$ .

For the present case  $L_e/D_{h_{in}} = 20$  and thus  $L_e = 3800 \mu\text{m}$ , which is much larger than the actual length of the inlet channel  $L' = 1500 \mu\text{m}$ , corresponding to a  $L'/D_{h_{in}} = 8.8$  (actually the reduced length of the inlet channels, which represents the

distance between the inlet and the edge of the mixing region, should be used instead thus leading to  $L'/D_{h_{in}} = 7.3$ ). Thus the non-FD case presents conditions far from a fully developed flow and, consequently, the resulting velocity profile is more blunt than the Poiseuille parabolic curve.

### Solver control

Most of the simulations were run with a steady solver. A second order discretisation scheme was used for all equations, as higher order discretization schemes were found to provide no appreciable differences. A sufficient number of iterations was performed to obtain residuals for all equations of less than  $10^{-13}$  and a stationary solution with iterations. Most of the times, equations residuals of  $10^{-5}$  or  $10^{-6}$  are considered sufficiently small to reach steady solutions in CFD problems. However, the monitor of some physical variables indicated that for the present case residuals of even  $10^{-7}$  were not sufficient to obtain stable solutions (leading to completely different mixing patterns than the converged ones), so that residuals should be driven to values less than  $10^{-13}$ . Practically many times, residuals were found to firstly decrease down to about  $10^{-8} - 10^{-7}$  (finding an unstable solution of the flow field), then to increase again (changing the flow pattern) and only after that to decrease down to  $10^{-13}$  (corresponding to a stable solution) [17]. The simulation for the FD case at  $\text{Re} = 480$  was also performed with a transient solver, but this indicated a steady flow.

### RESULTS

Figure 3 depicts velocity vectors (colored by the longitudinal velocity component, i.e.  $v_y$ ) at different cross-sections of the mixing channel for the non-FD case. It can be observed (Figure 3a) the formation of 2 pair of vortices (on the right- and left- hand sides) which initially are very similar. Moreover the flow field is symmetric with respect to the  $xy$  mid-plane. While proceeding along the mixing channel, the engulfment occurs as one stream tends to enter through the central part of the cross-section. This leads to an engulfment flow with a C-shaped pattern, i.e. displaying a) a mirror symmetry with respect to the  $xy$  mid-plane; b) no interchangeability between the two inlet fluids (see Figure 3d). This is also evident from the distribution of tracer concentration on the same planes reported in Figure 4. At the beginning of the mixing channel, the two fluids are well segregated (see Fig. 4a for  $y = -500 \mu\text{m}$ ); then the tracer, coming from the right-hand side, crosses the  $yz$  mid-plane near the center, whereas the stream coming from the left-hand side crosses the plane near the walls, thus originating a pair of vortices, as it can be evinced from Fig. 4d, with  $y = -2500 \mu\text{m}$ . The authors knowledge this kind of engulfment (with C-shape pattern or kidney-vortex structure) has not been observed previously in micro-mixer, even though it is known for other configurations, such as crossflow jets [18]. Additional simulations have shown that the fluid that tends to concentrate at the center of the mixing channel could be the red fluid, coming from the left-hand inlet channel, as reported here or, with equal probability, the blue fluid, coming from the right-hand side. For the non-FD case the  $\text{Re} = 480$  of the present results correspond to the onset of the engulfment as shown in our previous work [17].

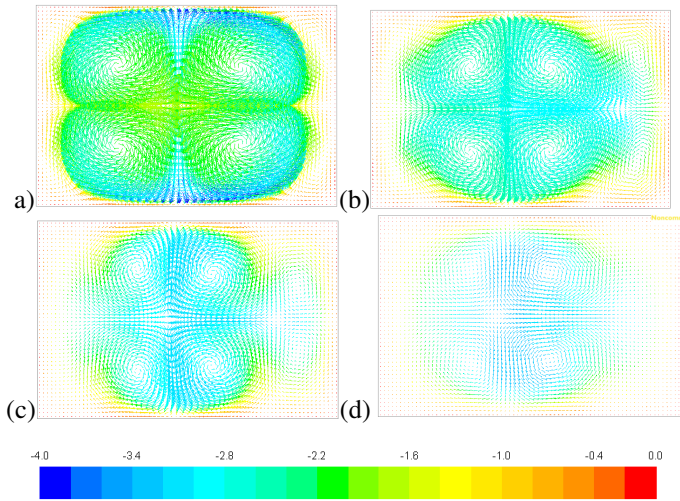


**Figure 3** - Velocity vectors on xz planes (coloured by  $v_y$ , m/s) for non-FD case at: (a)  $y = -500 \mu\text{m}$ ; (b)  $y = -1000 \mu\text{m}$ ; (c)  $y = -1500 \mu\text{m}$ ; (d)  $y = -2500 \mu\text{m}$ .  $Re = 480$ .

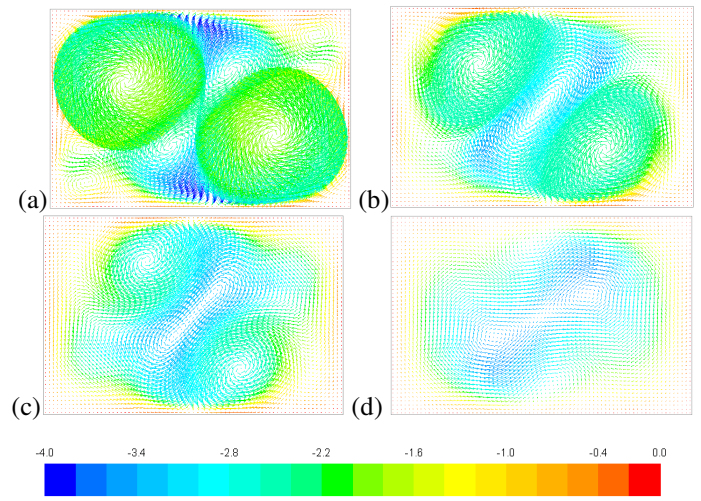


**Figure 5** - Velocity vectors on xz planes (coloured by  $v_y$ , m/s) for FD case at: (a)  $y = -500 \mu\text{m}$ ; (b)  $y = -1000 \mu\text{m}$ ; (c)  $y = -1500 \mu\text{m}$ ; (d)  $y = -2500 \mu\text{m}$ .  $Re = 480$ .

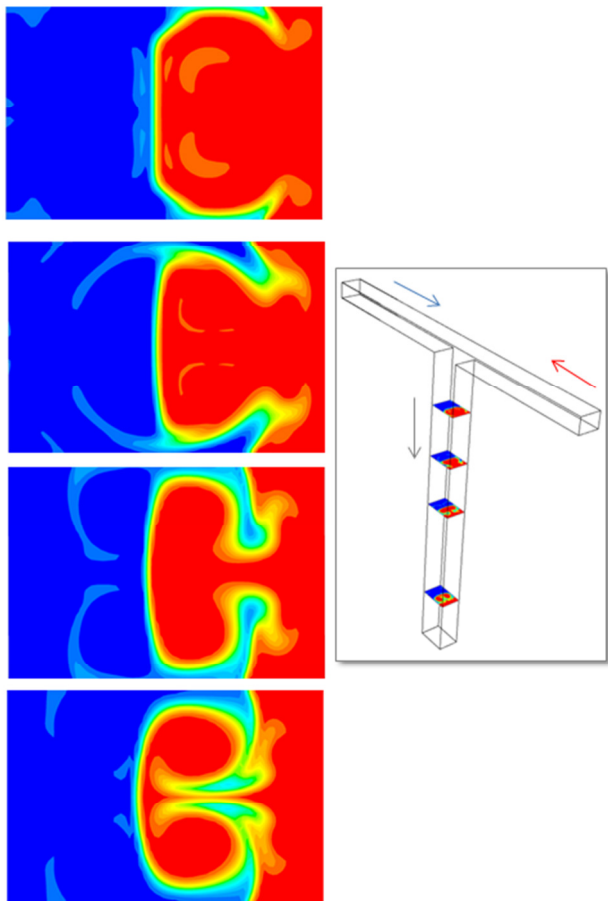


**Figure 4** - Tracer concentration distribution along the mixing channel for the non-FD case at: (a)  $y = -500 \mu\text{m}$ ; (b)  $y = -1000 \mu\text{m}$ ; (c)  $y = -1500 \mu\text{m}$ ; (d)  $y = -2500 \mu\text{m}$ .  $Re = 480$ .

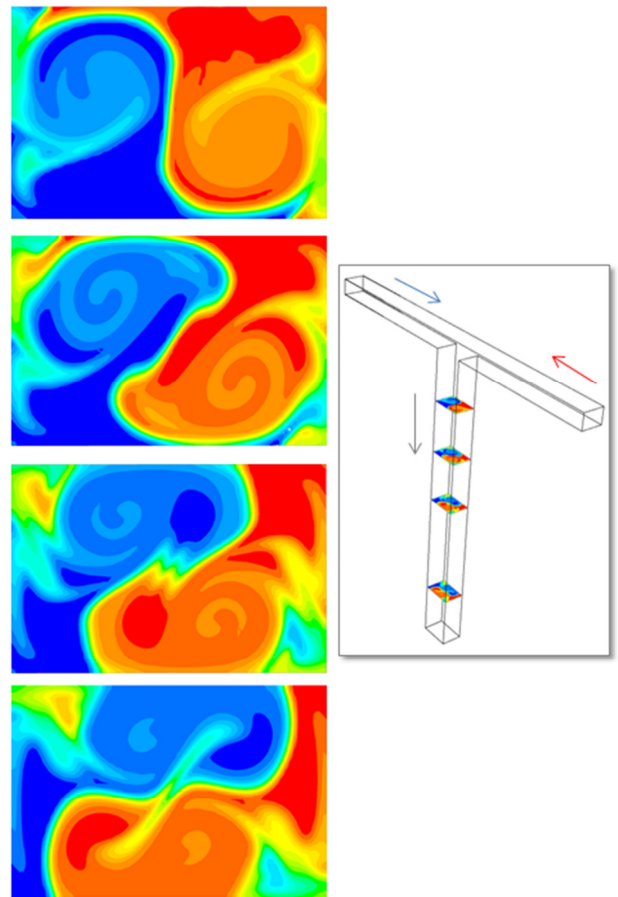


**Figure 6** - Tracer concentration distribution along the mixing channel for the FD case at: (a)  $y = -500 \mu\text{m}$ ; (b)  $y = -1000 \mu\text{m}$ ; (c)  $y = -1500 \mu\text{m}$ ; (d)  $y = -2500 \mu\text{m}$ .  $Re = 480$ .

For lower Re a laminar flow regime was observed resulting in a segregated flow.

Similarly Figure 5 reports velocity vectors for the FD case. It can be observed that in this case engulfment occurs as one stream enters preferentially below the xy mixer mid-plane, whereas the other stream enters above it, leading to a big pair of vortices and other minor vortical structures. Thus the flow is in the fully engulfment regime.

The engulfment for the FD case shows a S-shaped pattern, i.e. displaying a) a point symmetry with respect to the center of the cross section; b) interchangeability between the two inlet fluids. It was found that for the present micro-mixer, the engulfment occurred at much lower Reynolds number, i.e. around Re = 192 in case of FD case [17]. Moreover Re = 480 is also above the range of Reynolds numbers for which periodic instabilities were observed [9, 17]. For the present micro-mixer geometry such instabilities were found to occur between Re = 220 and Re = 400. However for higher Re, stable steady state solutions were found.

Figure 6 illustrates the distribution of the tracer at different cross sections along the mixing channel for the FD case, indicating that the engulfment patterns are similar to those observed by other researchers. For instance, the tracer distribution at  $y = -500 \mu\text{m}$  (Fig. 6a) is alike the S-shaped engulfment pattern observed experimentally by [4] and numerically by [6] for a different T-micro-mixer.

Figure 7 compares the tracer concentration distribution in the xy (horizontal) mid-plane for the non-FD and FD cases. It can be observed how the presence of a flat region in the inlet velocity profile (non-fully developed conditions) damps the mixing process. Moreover the FD case shows a symmetric pattern with respect to the yz mid-plane, whereas for the non-FD case the two streams are not interchangeable.

To compare the mixing efficiency in the two cases, a bulk concentration (also referred to as “cup mixing concentration” or “flow average concentration”), that is the flow-weighted mean concentration, is defined as:

$$\bar{c} = \frac{\langle cv \rangle}{\langle v \rangle}; \quad \langle cv \rangle = \frac{1}{A} \int_A cv \, dA; \quad \langle v \rangle = \frac{1}{A} \int_A v \, dA, \quad (4)$$

where the overbar indicates the cup mixing average, while the brackets denote the volume (i.e. un-weighted) average on a cross section of area A. The cup mixing is preferred over the more usual volume, average concentration, because it, describes the concentration that “one would measure if the tube were chopped off and if the fluid issuing forth were collected in a container and thoroughly mixed” [19]

In the same way, a bulk, or cup mixing, mean square concentration difference can be defined as:

$$\overline{(\Delta c)^2} = \frac{\langle (c - \bar{c})^2 v \rangle}{\langle v \rangle}; \quad \sigma_{cm}^2 = \overline{(\Delta c)^2} / \overline{(\Delta c)^2}_{\max}, \quad (5)$$

where its maximum value is used as a normalizing factor. Such maximum mean square concentration difference occurs when the two streams are completely unmixed (i.e.,  $c=0$  in half

of the cross section and  $c=1$  in the other half) we have:  $\overline{(\Delta c)^2}_{\max} = 1/4$ . For sake of convenience, it will be used the following definition of degree of mixing,

$$\delta_m = 1 - \sigma_{cm} \quad (6)$$

which varies from 0, when the two streams are perfectly unmixed, to 1, when they are completely mixed.

Figure 8 compares the degree of mixing, along the mixing channel in the FD case with that in the non-FD showing that it is much larger in the former. It can also be observed that in both cases as expected, the degree of mixing augments along the mixing channel. In the outlet section the degree of mixing for the FD case is  $\delta_m = 0.25$ , whereas it is just  $\delta_m = 0.15$  for the non-FD case, thus confirming the most effective mixing obtained with a parabolic inlet flow.

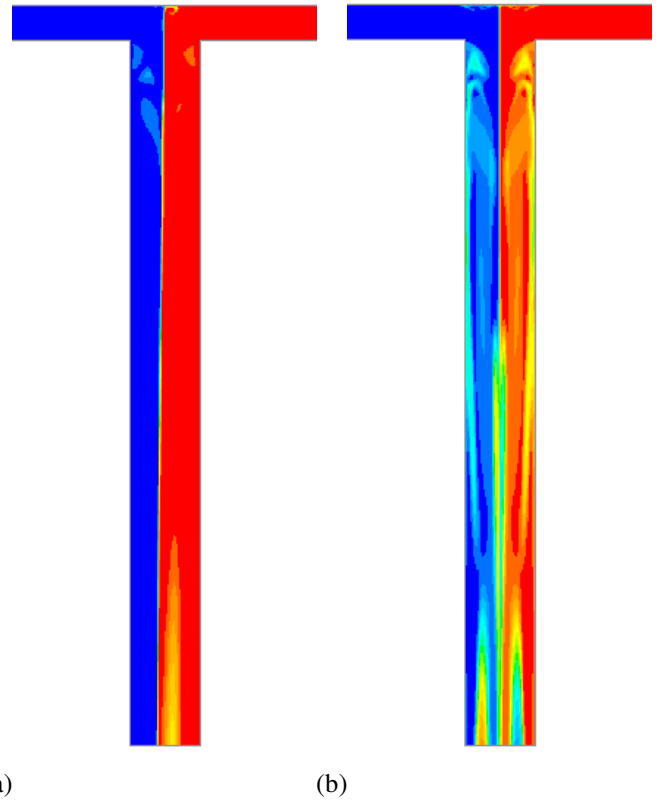


**Figure 7** - Tracer concentration distribution in the xy mid-plane for (a) non-FD case and (b) FD case (branches have been cut in the image). Re = 480.

## CONCLUSION

The effect of inlet flow conditions on the mixing process of a T-shaped micro-mixer has been investigated. In particular it was found that when fully developed conditions are ensured at the inlets, the engulfment occurs at relatively low Reynolds numbers and with typical S-shaped flow patterns. On the other hand, when the fluid flow at the confluence is non-fully

developed and presents even a small plug flow region at the center, engulfment occurs at much larger Reynolds numbers and with a C-shaped engulfment pattern (with the tracer crossing the mixing channel mid-plane either near the center or at the walls). This is also characterised by a much lower mixing efficiency.

Therefore the issue of fully (or not) developed flow at inlets may affect strongly the mixing process, thus it should be taken into account for the design of mixers, especially when there can be limitations on the length of the inlet channels, as for instance in case of micro-channel networks.

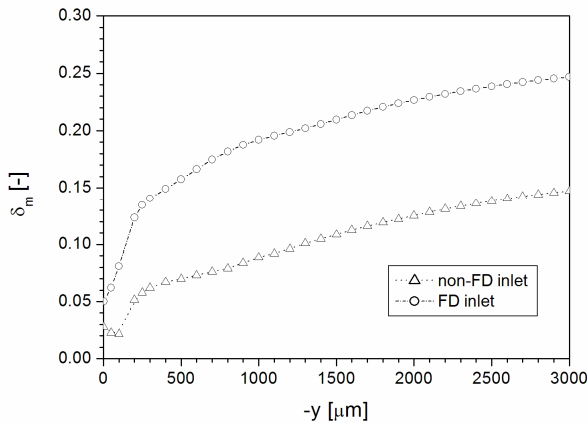


**Figure 8** - Degree of mixing along the mixing channel for the non-FD and the FD cases.  $Re = 480$ .

## REFERENCES

- [1] Kumar V., Paraschivoiu M., and Nigam K.D.P., Single-phase fluid flow and mixing in microchannels, *Chemical Engineering Science*, Vol. 66, 2011, pp. 1329-1373.
- [2] Bothe D., Lojewski A., and Warnecke H.-J., Computational analysis of an instantaneous chemical reaction in a T-microreactor, *American Institution of Chemical Engineers Journal*, Vol. 56, 2010, pp. 1406-1415.
- [3] Bökenkamp D., Desai A., Yang X., Tai, Y. Marzluff E., and Mayo S., Microfabricated silicon mixers for submillisecond quench-flow analysis, *Analytical Chemistry*, Vol. 70, 1998, pp. 232-236.
- [4] Hoffmann M., Schlüter M., and Rübiger N., Experimental investigation of liquid-liquid mixing in T-shaped micro-mixers using  $\mu$ -LIF and  $\mu$ -PIV, *Chemical Engineering Science*, Vol. 61, 2006, pp. 2968-2976.
- [5] Engler M., Kockmann N., Kiefer T., and Woias P., Numerical and experimental investigations on liquid mixing in static micromixers, *Chemical Engineering Journal*, Vol.101, 2004, pp. 315-322.
- [6] Bothe D., Stemich C., and Warnecke H.-J., Fluid mixing in a T-shaped micro-mixer, *Chemical Engineering Science*, Vol. 61, 2006, pp. 2950-2958.
- [7] Soleymani A., Yousefi H., Turunen I., Dimensionless number for identification of flow patterns inside a T-micromixer, *Chemical Engineering Science*, Vol. 63, 2008, pp. 5291-5297.
- [8] Reddy Cherlo S.K., and Pushpavanam S., Effect of depth on onset of engulfment in rectangular micro-channels, *Chemical Engineering Science*, Vol. 65, 2010, pp. 6486-6490.
- [9] Dreher S., Kockmann N., and Woias P., Characterization of laminar transient flow regimes and mixing in T-shaped micromixers, *Heat Transfer Eng.* 30, 2009, pp. 91-100.
- [10] Soleymani A., Kolehmainen E., and Turunen I., Numerical and experimental investigations of liquid mixing in T-type micromixers, *Chemical Engineering Journal*, Vol. 135, 2008, pp. S219-S228.
- [11] Aoki N., Umei R., Yoshida A., and Mae K., Design method for micromixers considering influence of channel confluence and bend on diffusion length, *Chemical Engineering Journal*, Vol.167, 2011, pp. 643-650.
- [12] Hussong J., Lindken R., Pourquie M., and Westerweel J., Numerical study on the flow physics of a T-shaped micro mixer, in: B.V. M. Ellero et al. (eds.), *IUTAM Symposium on Advances in Micro- and Nanofluidics*, IUTAM Bookseries 15, Springer Science + Business Media, 2009.
- [13] Ottino J.M., and Wiggins S., *Introduction: mixing in microfluidics*, Philos. Trans. R. Soc. London, Ser. A 362,2004, pp. 923-935.
- [14] Chatwin P.C., and Sullivan P.J., The effect of aspect ratio on the longitudinal diffusivity in rectangular channels, *Journal of Fluid Mechanics*, Vol. 120, 1982, pp. 347-358.
- [15] Happel J., and Brenner H., *Low Reynolds Number Hydrodynamics*, Prentice Hall, 1965; Eq. (2-5.24).
- [16] Dombrowski N., Foumeny E.A., S. Ookawara, and A. Riza, The influence of Reynolds number on the entry length and pressure drop for laminar pipe flow, *Canadian Journal of Chemical Engineering*, Vol. 71, 1993, pp. 472-476.
- [17] Galletti C., Roudgar M., Brunazzi E., and Mauri R., Effect of inlet conditions on the engulfment pattern in a T-shaped micro-mixer *Chemical Engineering Journal*, Vol. 185-186, 2012, pp. 300-313
- [18] Haven B.A., and Kurosaka M., Kidney and anti-kidney vortices in crossflow jets. *Journal of Fluid Mechanics*, Vol. 352, 1997, pp 27-64
- [19] Bird R.B., Stewart W.E., and Lightfoot E.N., *Transport Phenomena*, Wiley, 1960, pp. 297 and 641.